Investigating the Spatio-temporal Variability of Climate and Its Impact on Wind Power Generation and Management

Liang-Chun Chen[a], Ying-Yi Lai[b], Chien-Pang Lee[c*]

[a] Department of Information Management, National Taipei University of Nursing and Health Sciences, Taipei City, Taiwan

[b] Master's Program in Offshore Wind Energy Engineering, National Kaohsiung University of Science and Technology, Kaohsiung City, Taiwan

[c] Department of Public Finance and Tax Administration, National Taipei University of Business, Taipei City, Taiwan

*Corresponding Author:

Chien-Pang Lee

Department of Public Finance and Tax Administration,

National Taipei University of Business

No. 321, Sec. 1, Jinan Rd., Taipei 10051, Taiwan

Tel: +886-2-2322-6444

E-mail: chienpang@ntub.edu.tw

Abstract

Green energy has become a central focus for power generation around the world. Many companies now require green energy in their production processes, which has led many countries to invest in its development. The Taiwan Strait is considered one of the top locations for offshore wind power in the world. Since 2018, Taiwan has actively promoted the development of offshore wind power. Wind power generation is intermittent and affected by climate variability, which creates significant challenges for its stability and reliability. This study collected wind power generation data from the Changhua Coastal Wind Power Station between May 2021 and June 2022. Climate data, including wind speed and wind direction, were obtained from nearby weather stations and were used to generate monthly and seasonal wind rose diagrams. Statistical analysis indicated that wind power generation in summer represented just 9.81% of the annual total, while winter accounted for 46.00%. A 24-hour generation analysis showed that the highest hourly generation percentage in summer was only 17.82%, while in winter, it consistently remained above 50% during most periods. These findings reveal a notable seasonal and daily variation in wind power generation, mainly influenced by wind speed and direction changes. To minimize the effects of periods with low power generation and to meet the peak electricity demand during the summer, it is crucial to implement large-scale energy storage systems along with effective power dispatch and management strategies. This approach will help ensure grid stability and reliability.

Keywords: Wind power generation, Green energy, Climate data, Spatio-temporal variability, Wind rose diagram.

1. Introduction

As the world transitions towards a more sustainable energy landscape, the role of renewable energy sources, including wind power, has become increasingly significant. This shift is driven by the growing awareness of environmental sustainability and the need to reduce the reliance on traditional, polluting power generation methods.

Wind power generation is one of the most promising sources of renewable energy. However, it faces significant challenges, including fluctuations, intermittency, and unstable power generation. To enhance the reliability and efficiency of wind power, further comprehensive research and discussions are necessary.

Despite these challenges, wind energy remains a renewable and sustainable energy source. Recently, advancements in wind energy technology have gained increasing attention due to their low operational and maintenance costs, minimal land footprint, and high flexibility.

Most wind farms have been established in remote areas, far from the primary power grid. The power systems connected to these wind farms are often fragile, making them highly susceptible to power fluctuations caused by wind power generation. Additionally, insufficient wind speeds can significantly reduce power generation, highlighting the need for further technological improvements. However, offshore wind conditions are more stable than land due to the absence of obstacles and the smoother wind flow over the ocean. As a result, offshore wind power generation offers higher economic benefits and better capacity utilization [1].

The waters of the Taiwan Strait have been recognized by the international engineering consultancy 4C Offshore as one of the world's best offshore wind sites, with an estimated potential of several tens of gigawatts (GW) [2]. In line with global trends in renewable energy development, Taiwan has been actively expanding offshore wind farms with the long-term goal of establishing an independent power grid. However, Taiwan experiences significant seasonal variations in wind conditions. During winter, the northeast monsoon brings strong and high-speed winds, whereas in summer, the southwest monsoon results in significantly lower wind speeds [3].

The literature has also highlighted the instability of wind power generation and proposed corresponding mitigation strategies. For instance, Obara et al. [4] and Tooryan et al. [5] pointed out that wind power instability is most pronounced at night and during summer when supply-demand imbalances arise due to fluctuating power generation. In power systems, the intermittency of renewable energy can lead to frequency deviations among generating units, a phenomenon known as power frequency chasing. In severe cases, this instability may result in generator shutdowns, posing a significant risk to the power grid system.

The integration of energy storage systems (ESS) into the grid has been proposed as a solution to address this issue. Due to their rapid response capabilities, ESS can promptly compensate for fluctuations in electricity demand, thereby stabilizing grid frequency [6] and preventing generator shutdowns. Furthermore, ESS can be charged when renewable energy generation is active and, under normal conditions, should remain near full capacity in grid-connected mode to meet disaster preparedness requirements. This enables ESS to complement renewable energy sources, enhancing grid stability and reducing carbon emissions.

Taiwan's power grid operates as an islanded system, meaning it must be self-sufficient in meeting its electricity demand. To ensure a secure and reliable power supply, the generation sector must develop accurate power demand forecasts. To enhance economic and energy efficiency [7], the grid system must be appropriately integrated with energy storage systems (ESS) to mitigate the intermittency of renewable energy sources and increase operational flexibility.

Accurate wind speed analysis and practical wind energy simulations can significantly improve the grid integration capability of wind power, thereby reducing operational costs for wind farms. Furthermore, precise forecasting provides a scientific basis for wind farm generation planning, enabling the development of optimized ESS charging and discharging strategies. This, in turn, helps reduce curtailment incidents and minimizes the duration of wind power curtailment [8].

However, wind is often considered one of the most challenging parameters to predict in meteorological systems, primarily due to its intermittent and nonlinear characteristics. Wind exhibits substantial variations over wide temporal and spatial scales in real-world atmospheres, mainly driven by underlying atmospheric fluid dynamics. The quasi-random behavior of wind is influenced by the interplay among large-scale forcing mechanisms (such as pressure differences and temperature gradients), the Earth's rotation, and local surface features [9].

Nevertheless, numerous studies have attempted to forecast wind power generation by evaluating wind speed and direction. For instance, Jin et al. [10] analyzed the correlation and significance of wind speed and direction. Furthermore, spatially correlated wind energy data can be obtained along with power grid fluctuations. This enables a more accurate assessment and correction of frequency deviations and capacity outputs caused by the natural intermittency of wind power generation. Wu [11] employed wind speed and wind direction data to analyze wind turbine power generation, thereby establishing a historical database. By integrating detailed forecasting data from other regions in Taiwan, a reliable basis for energy forecasting can be achieved.

Wind power generation has become an indispensable method to enhance and manage the stability of Taiwan's power grid. However, to avoid power shortages resulting from the inherent instability of wind power, investigating the impact of wind speed and wind direction on wind power generation in Taiwan has emerged as a critical issue. This study analyzes existing onshore wind power data from Taiwan to examine how wind speed and direction affect power generation at different times and quantify the extent of impact caused by extreme climate conditions. By analyzing wind climate data alongside power generation data—using monthly, seasonal, and hourly average wind speed statistics and monthly and seasonal wind direction statistics—this study aims to elucidate the influence of wind on wind power generation.

Since wind speed and direction exert varying effects on wind power generation, it is essential to understand the differences between peak and off-peak periods of wind power generation and to coordinate grid supply during low power generation periods. This study investigates whether deploying energy storage systems during high power generation periods and expanding their capacity can mitigate the effects of low wind conditions or weak wind speeds that lead to power generation troughs, thereby promptly compensating for electricity demand gaps. Consequently, the objectives of this study are as follows:

a. To investigate the impact of spatiotemporal climate data on wind power generation.
b. To examine the seasonal differences between peak and off-peak wind power generation periods.
c. To assess the feasibility of integrating wind power generation with the energy storage industry.

The structure of this paper is organized as follows: Section 2 introduces the dataset and analysis methodology, Section 3 presents the statistical analysis results, Section 4 offers a discussion of the findings, and Section 5 concludes the study.

2. Materials and Methods

2.1 Dataset

This study obtained wind power generation and climate data from the Taiwan Power Company website and the publicly available observational data provided by the Central Weather Administration of Taiwan, respectively. The analysis focuses on a case study involving the real-time power generation of the Changhua Coastal Wind Power Station, updated every 10 minutes, and the climate data from the Sian Si weather station. The locations of the Changhua Coastal Wind Power Station and the Sian Si weather station are shown in Figure 1. The data collection period spans from May 23, 2021, to June 7, 2022, and includes hourly power generation data, hourly wind speed, and wind direction data.

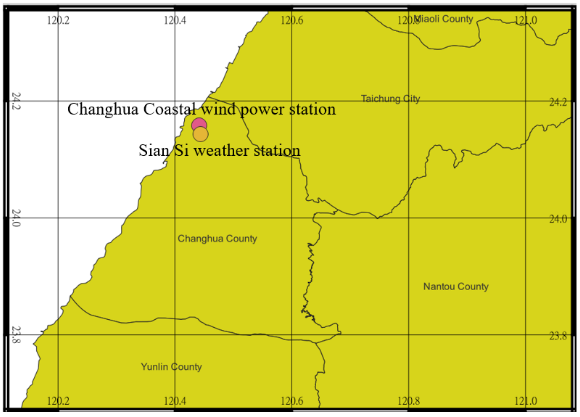

Fig. 1. Location of the Changhua Coastal Wind Power Station and Sian Si Weather Station.

2.2 Data Organization and Analysis Process

2.2.1 Data Pre-treatment

Since the wind power generation and climate data originate from different sources, the first step was to merge the datasets based on their collection times. For example, the wind power generation data recorded at 10:00 AM on May 23, 2021, were combined with the climate data from the same timestamp to form a single observation. Next, to understand the variations in wind direction and wind speed across different seasons, months, and hours, the dataset extracted the month, day, and hour from the original timestamps. Furthermore, a column for the season was added to the dataset. The seasons were defined according to common usage in Taiwan: spring (March-May), summer (June-August), fall (September-November), and winter (December-February).

Additionally, due to the inherent instability of wind and its seasonal variations, a new column titled "Wind Speed Description" has been added to categorize wind speeds into four classifications: no wind, low wind speed, median wind speed, and high wind speed. Based on the criteria referenced in [12], wind speed was defined

ISSN: 0067-3064

as follows: no wind: 0 (m/s); low wind speed: below 5 (m/s); median wind speed: between 5 (m/s) and 10 (m/s); and high wind speed: above 10 (m/s). A column classifying net power generation was also added, with categories defined as low, median, and high net power generation. Specifically, low power generation was defined as net power generation below 25% of the device capacity, median power generation as net power generation between 25% and 50% of the device capacity, and high power generation as net power generation above 50% of the device capacity.

After this processing, the final dataset comprised 12 variables: Year, Month, Day, Hour, Season, Device capacity, Net power generation, Net power generation classification, Wind direction, Wind direction angle description, Wind speed, and Wind speed description. A portion of the dataset is shown in Table 1.

Table 1. Parts of the dataset.

Year	Month	Day	Hour	Season	Device capacity (MW)	Net power generation (MW)	Net power generation classification	Wind direction	Wind direction angle description	Wind speed (m/s)	Wind speed description
2021	5	23	10	Spring	71.2	3.1	Low	273	W-N	2.6	Low
2021	5	23	11	Spring	71.2	5.5	Low	279	W-N	3.1	Low
2021	5	23	12	Spring	71.2	5.6	Low	259	S-W	3.6	Low
2021	5	23	13	Spring	71.2	6.3	Low	276	W-N	3.4	Low
2021	5	23	14	Spring	71.2	4.9	Low	281	W-N	3.7	Low
2021	5	23	15	Spring	71.2	4	Low	268	S-W	2.9	Low
2021	5	23	16	Spring	71.2	1.6	Low	251	S-W	1.9	Low
2021	5	23	17	Spring	71.2	0	Low	242	S-W	1.3	Low
2021	5	23	18	Spring	71.2	0	Low	239	S-W	1.7	Low
2021	5	23	20	Spring	71.2	0	Low	233	S-W	1.7	Low

2.2.2 Main Analysis Process

The analysis process in this study was divided into three main steps, which are described as follows:

- Step 1: Data Organization and Descriptive Statistics for Wind Speed and Wind Direction

Descriptive statistical analyses were performed on the dataset's wind speed and wind direction data, including hourly, monthly, and seasonal statistics.

- Step 2: Plotting Wind Rose Diagrams for Wind Speed and Wind Direction

Wind rose diagrams for each month and for the entire year were generated using R language [13]. These diagrams clearly visualize the changes in wind direction and wind speed over time.

- Step 3: Comparison of Wind Speed and Net Power Generation

The average values corresponding to low, median, and high net power generation for the wind farm capacity were calculated. In addition, the maximum wind speed and wind direction for each month were recorded and compared with the net power generation to explore the relationship between these variables.

3. Results

3.1 Descriptive Statistics of Wind Speed and Wind Direction

Table 2 presents the complete observational dataset collected from May 23, 2021, to June 7, 2022, along with the monthly statistical summary of the observations. However, due to potential issues with data completeness—such as missing records or instrument malfunctions—the valid observational data, after excluding the affected entries, are summarized in Table 3.

Table 4 presents the statistical analysis of the average wind speed and its distribution. It can be observed from Table 4 that the average wind speeds in December, January, and February all exceed the annual average of 3.26 (m/s), indicating that the highest average wind speeds occur between late fall and winter.

ISSN: 0067-3064

In addition, the maximum wind speed is recorded in October, with values exceeding 12 (m/s). The overall wind speed distribution for the year is characterized by low wind speed accounting for 82.33%, median wind speed for 17.55%, and high wind speed for 0.12%.

Table 2. Summary statistics of raw observational records for each month from May 23, 2021, to June 7, 2022.

Month	**Jan.**	**Feb.**	**Mar.**	**Apr.**	**May.**	**Jun.**
Sample size	673	662	710	687	890	888
Month	**Jul.**	**Aug.**	**Sep.**	**Oct.**	**Nov.**	**Dec.**
Sample size	753	785	749	739	690	693

Table 3. Summary statistics of valid observational records for each month from May 23, 2021, to June 7, 2022.

Month	**Jan.**	**Feb.**	**Mar.**	**Apr.**	**May.**	**Jun.**
Sample size	652	631	689	675	838	852
Month	**Jul.**	**Aug.**	**Sep.**	**Oct.**	**Nov.**	**Dec.**
Sample size	714	714	703	723	680	666

Figure 2 shows the distribution of average wind speeds by hour. It can be observed that, regardless of the season, wind speeds begin to increase from 08:00 in the morning, peak at 15:00, and then decline after 16:00. Higher wind speeds characterize the period from morning to afternoon.

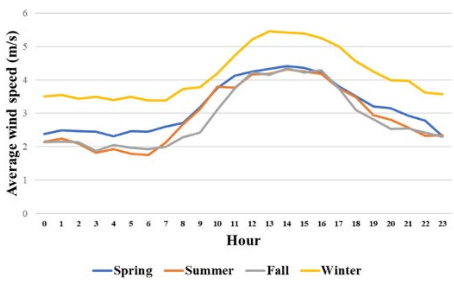

Fig. 2. Distribution of wind speed by hour and season.

Table 4. Statistical analysis of average wind speed and wind speed distribution.

Month	Average wind speed (m/s)	Max wind speed (m/s)	SD of wind speed (m/s)	Max wind speed's direction	Low wind speed (< 5 m/s)	Median wind speed (5 -10m/s)	High wind speed (>10 m/s)
Jan.	3.99	8.7	1.54	N-E	72.85%	27.15%	0%
Feb.	4.37	9.7	1.69	N-E	66.40%	33.60%	0%
Mar.	3.19	8.2	1.75	N-E	84.16%	15.84%	0%
Apr.	3.29	8.2	1.81	N-E	82.07%	17.93%	0%
May.	3.10	8.4	1.62	N-E	86.63%	13.37%	0%
Jun.	2.99	8	1.69	S-W	86.03%	13.97%	0%
Jul.	3.21	10.6	2.23	N-E	80.39%	18.77%	0.84%
Aug.	2.59	9.2	1.53	S-W	93.00%	7.00%	0%
Sep.	2.24	9.9	1.52	N-E	95.45%	4.55%	0%
Oct.	3.10	12.1	2.00	N-E	81.33%	18.26%	0.41%
Nov.	3.22	8	1.67	N-E	84.71%	15.29%	0%
Dec.	4.09	10.3	1.80	N-E	70.42%	29.43%	0.15%
Average	3.26	9.27	1.74		82.33%	17.55%	0.12%

Note: SD represents standard deviation.

Table 5 presents the monthly distribution statistics of wind direction. Table 5 shows the average distribution for the entire year: N-E at 57.51%, E-S at 5.54%, S-W at 26.12%, W-N at 8.51%, and no wind at 2.32%. When the data are examined by season (see Table 6), the overall wind direction is primarily dominated by the northeast monsoon. Specifically, the northeast monsoon accounts for 67.92% in spring, 59.92% in fall, and 97.43% in winter. Notably, from November to February, the northeast monsoon averages over 80%, indicating a stable northeast wind during winter, with only 0.05% classified as the southwest monsoon. In contrast, during summer, the predominant wind direction shifts to the southwest monsoon, which constitutes 66.14% of the summer wind distribution; however, wind directions are less consistent in summer, with the remaining directions accounting for over 31% of the distribution.

Table 5. Monthly distribution statistics of wind direction analysis.

Month	E-S	N-E	S-W	W-N	No wind
Jan.	0.15%	98.47%	0%	1.23%	0.15%
Feb.	0.48%	97.94%	0%	1.27%	0.32%
Mar.	4.07%	73.11%	11.48%	8.43%	2.91%
Apr.	1.78%	68.44%	16.00%	9.33%	4.44%
May.	3.94%	63.25%	26.25%	4.53%	2.03%
Jun.	7.63%	10.21%	75.47%	4.69%	2.00%
Jul.	7.28%	16.95%	52.52%	19.75%	3.50%
Aug.	13.03%	6.30%	68.63%	10.50%	1.54%
Sep.	13.94%	31.15%	26.17%	24.47%	4.27%
Oct.	7.88%	63.90%	15.35%	10.51%	2.35%
Nov.	2.65%	85.44%	2.79%	6.03%	3.09%
Dec.	1.95%	95.95%	0.15%	0.90%	1.05%
Average	5.54%	57.51%	26.12%	8.51%	2.32%

Table 6. Seasonal distribution statistics of wind direction analysis.

Season	E-S	N-E	S-W	W-N	No wind
Spring	3.32%	67.92%	18.49%	7.22%	3.04%
Summer	9.21%	11.10%	66.14%	11.23%	2.32%
Fall	8.21%	59.92%	14.91%	13.72%	3.23%
Winter	0.87%	97.43%	0.05%	1.13%	0.51%

Figures 3 and 4 display the wind rose diagrams for the entire year and for each season, respectively. In contrast, the monthly wind rose diagrams are provided in Supplement Fig. 1. The Figures show that the prevailing wind direction is mainly from the northeast monsoon during winter. Additionally, the proportion of high wind speeds (greater than 10 m/s) from this direction is higher than winds from other directions. In contrast, the wind direction is less consistent during summer, and the occurrence of high wind speeds (>10 m/s) is less concentrated in a specific direction. As September transitions into the fall-winter period, the northeast monsoon is markedly strengthening. Throughout winter, the wind is consistently dominated by the northeast monsoon with a stable direction, achieving over 80%

ISSN: 0067-3064

of the wind distribution regardless of day or night. Moreover, a comparison of the diurnal wind rose diagrams reveals that, in spring and fall, daytime wind speeds are higher than nighttime speeds. Although the southwest monsoon generally dominates summer, the wind direction is less fixed, resulting in a lower wind direction concentration than in winter.

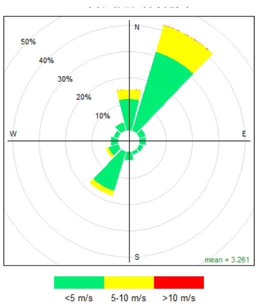

Fig. 3. Annual average wind speed rose diagram.

(a)

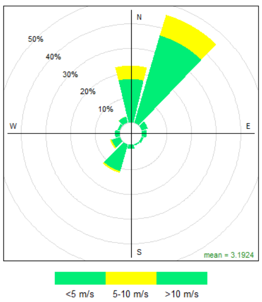

(b)

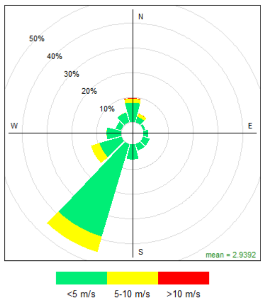

(c)

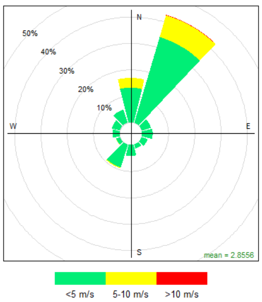

(d)

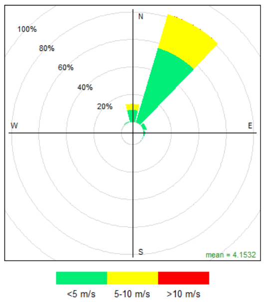

Fig. 4. Seasonal wind speed rose diagrams: (a) Spring; (b) Summer; (c) Fall; (d) Winter.

3.2 Descriptive Statistics of Power Generation

Table 6 presents the statistical summary of the monthly power generation ratios at the wind power station. It can be observed from Table 6 that the proportion of low net electricity generation reached its peak in June at 91.31%. As fall commences, the distribution of low net power generation decreases while the proportion of high net power generation increases. In September, during summer, high net power generation accounts for only 6.12%; however, this proportion rises significantly to 43.97% in November, indicating an increase in high net power generation during the fall and winter. From December to February, the high net power generation ratio ranges between 67.42% and 70.09%, with the proportion of low net power generation at a minimum of 15.80%. Notably, the highest high net power generation ratio is recorded in January at 70.09%. On an annual basis, the average distribution is 59.41% for low net power generation, 10.07% for median net power generation, and 30.52% for high net power generation.

When analyzed by season, the differences become even more pronounced (Table 7). Table 7 shows that the proportion of low net power generation is highest in summer at 87.85%, while high net power generation does not exceed 30% in spring and summer. In the fall, the data are less distinct, with the low net power generation proportion decreasing to 63.30% and high net power generation increasing to 27.97%. The contrast is even more evident in the winter, with low net power generation accounting for only 18.78% and high net power generation reaching 69.11%.

Table 6. Monthly power generation statistics.

Month	Low net power generation	Median net power generation	High net power generation
Jan.	15.80%	14.11%	70.09%
Feb.	18.07%	12.04%	69.89%
Mar.	65.55%	11.63%	22.82%
Apr.	54.67%	12.15%	33.19%
May.	65.51%	12.29%	22.20%
Jun.	91.31%	7.51%	1.17%
Jul.	81.23%	9.10%	9.66%
Aug.	90.34%	6.44%	3.22%
Sep.	91.18%	2.70%	6.12%
Oct.	56.98%	8.85%	34.16%
Nov.	41.18%	14.85%	43.97%
Dec.	22.37%	10.21%	67.42%
Average	59.41%	10.07%	30.52%

Note: "Low net power generation" indicates that the net power generation is below 25% of the device capacity; "Median net power generation" indicates that the net power generation is between 25% and 50% of the device capacity; "High net power generation" indicates that the net power generation exceeds 50% of the device capacity.

Table 7. Seasonal power generation statistics.

Season	Low net power generation	Median net power generation	Hight net power generation
Spring	62.20%	12.04%	25.76%
Summer	87.85%	7.68%	4.47%
Fall	63.30%	8.74%	27.97%
Winter	18.78%	12.11%	69.11%

4. Discussion

4.1 Power Analysis and Seasonal Statistics

When analyzing the differences in net power generation solely by season, it can be observed that the net power generation proportions of the power station are 22.21% in spring, 9.81% in summer, 21.99% in fall, and 46.00% in winter, as shown in Figure 5. Therefore, during summer, the net power generation is insufficient to provide a stable power supply, with the majority of power generation provided during spring, fall, and winter.

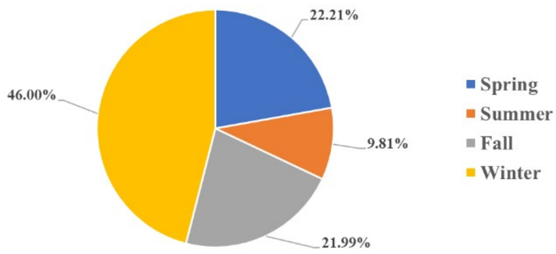

Fig. 5. Seasonal net power generation proportions.

4.2 Power Generation Statistics by Month and Hour

Figures 6 and 7 illustrate the hourly distribution of average power generation for the entire year and each season, respectively. The detailed monthly data are provided in Supplement Fig. 2 and Supplement Fig. 3. The annual average distribution indicates that at 09:00, the total power generation percentage is 28.44%. In response to the increase in daytime wind speeds, the total power generation percentage gradually rises, reaching a peak of 43.40% at 16:00. During the nighttime, from 18:00 to 06:00, the power generation percentage ranges between 20% and 39%. Overall, the lowest power generation levels are concentrated between May and September; specifically, in May, the highest power generation occurs at 14:00 at 35.55%, in June at 14:00 at 18.24%, in July at 15:00 at 22.65%, in August at 13:00 at 15.97%, and in September at 16:00 at 29.55%. Thus, from May to September, the maximum hourly power generation generally does not exceed 25% of the device capacity, indicating that power generation remains low for extended periods.

In contrast, the highest average maximum power generation occurs from October to February. Under the influence of the northeast monsoon, power generation is relatively more stable compared to May–September, with a marked increase beginning in October. Specifically, the maximum power generation in October is recorded at 17:00 at 44.95%, in November at 16:00 at 63.03%, in December at 17:00 at 87.36%, in January at 15:00 at 81.83%, and in February at 19:00 at 71.53%. Collectively, from October to February, the maximum hourly power generation exceeds 40% of the device capacity, reaching up to 80% in some instances, which indicates that this period is characterized by median to high power generation.

When discussing the seasonal differences by hour, the average highest power generation occurs in spring from 10:00 to 19:00, peaking at 14:00 with 35.70%. In comparison, the average power generation during nighttime and midnight remains above 20% of the device capacity. In summer, from 09:00 to 22:00, the peak average power generation occurs at 16:00 at 17.82%, with nighttime and midnight averages ranging only between 6% and 10% of the device capacity. In fall, from 09:00 to 18:00, the highest average power generation is observed at 16:00 at 44.26%, with nighttime and midnight averages maintaining at or above 15% of the device capacity. In winter, the average power generation remains above 50% of the device capacity throughout all periods (00:00 to 23:00), with the highest average power generation occurring at 17:00 at 80.71%.

Based on the seasonal hourly statistics of the Changhua Coastal Wind Power Station, it is evident that the overall average power generation in summer is the lowest and less stable, with most periods characterized by low power generation. In contrast, winter consistently exhibits high and stable power generation across all periods.

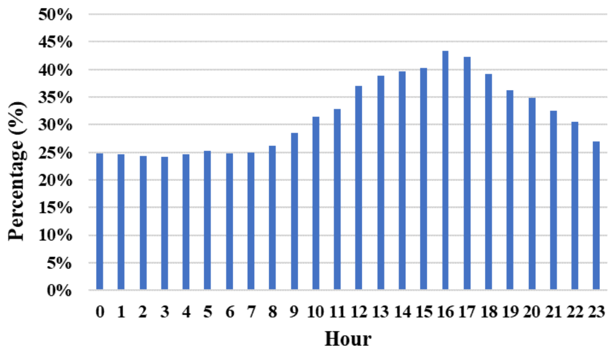

Fig. 6. Hourly average power generation percentage for the entire year.

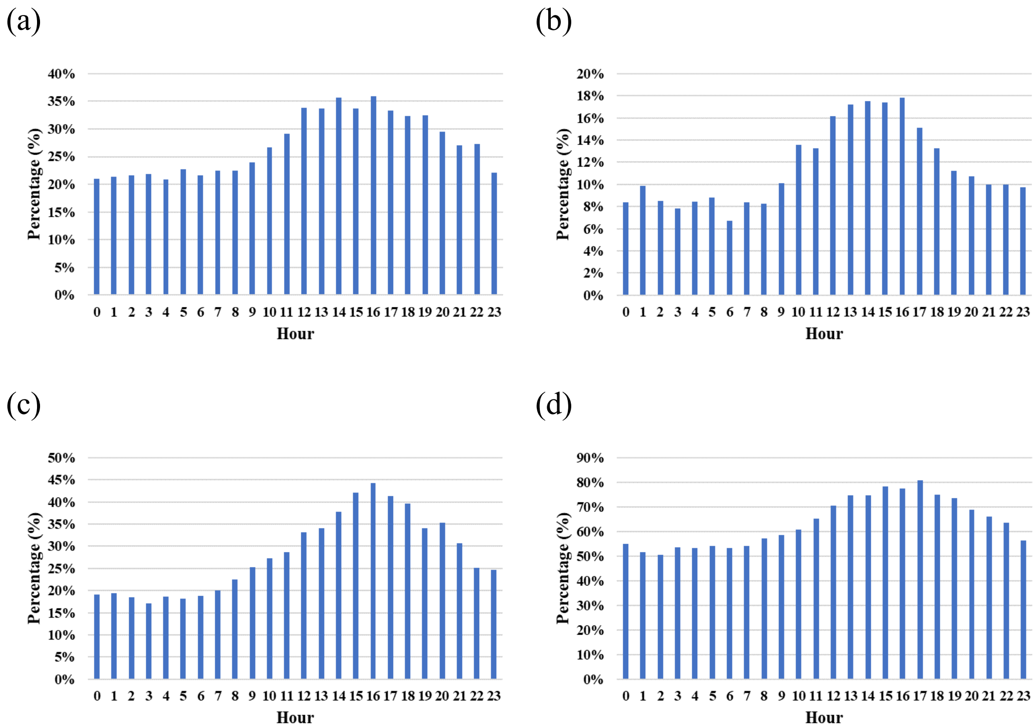

Fig. 7. Seasonal hourly average power generation percentage: (a) Spring; (b) Summer; (c) Fall; (d) Winter.

4.3 Analysis and Statistics of Power Generation and Wind Direction

Table 8 presents the wind direction and net power generation statistics. Over the entire year, in spring, the net power generation was attributed to 6.35% from the southwest wind and 92.47% from the northeast wind, while contributions from the southeast and northwest winds did not exceed 2%. In summer, 70.82% of the net power generation was produced by the southwest wind, followed by 19.94% from the northeast wind, with contributions from the southeast and northwest winds not exceeding 10%. In fall, 96.60% of the net power generation was generated by the northeast wind, followed by 1.81% from the northwest wind, while contributions from the southeast and southwest winds did not exceed 3%. In winter, the net power generation was overwhelmingly dominated by the northeast wind, accounting for 99.87%, with contributions from the southeast and northwest winds not exceeding 1%. On an annual basis, the power station's net power generation was produced primarily by the northeast wind (89.67%), followed by the southwest wind (8.65%). These results indicate that this wind farm's stable net power generation relies heavily on the northeast wind during the fall and winter seasons.

Table 8. Statistics of wind direction and net power generation.

Season	E-S	N-E	S-W	W-N	No wind
Spring	0.27 %	92.47%	6.35%	0.83%	0.09%
Summer	3.71%	19.94%	70.82%	5.49%	0.03%
Fall	0.22%	96.60%	1.35%	1.81%	0.02%
Winter	0.01%	99.87%	0.00%	0.12%	0.00%
Average	0.48%	89.67%	8.65%	1.17%	0.03%

4.4 Scatter Relationship between Power Generation and Wind Speed

Figure 8 is a scatter plot illustrating the relationship between wind speed and net power generation at the power station, with wind speed on the x-axis and net power generation on the y-axis. The scatter plot shows that the wind speeds at the power station are concentrated between 2 (m/s) and 8 (m/s), indicating that the wind field is characterized by low to median wind speeds. Moreover, there is a positive correlation between wind speed and net power generation; as wind speed increases, net power generation also increases. This further confirms the significant influence of wind speed on net power generation.

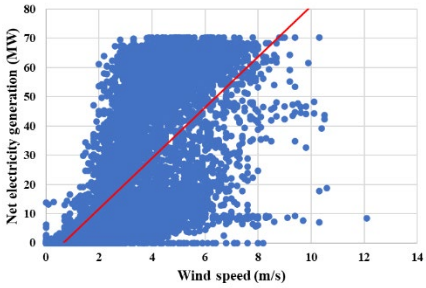

Fig. 8. Scatter plot of wind speed and net power generation.

5. Conclusion

This study analyzed the monthly, seasonal, and annual average wind speed and wind direction statistics of the wind power station and examined the relationships between power generation, wind speed, and wind direction across different periods of the two wind fields. The following conclusions were drawn:

a. Wind Speed Analysis:

The annual wind speed distribution at the power station is predominantly characterized by low wind speeds, with low wind speed occurrences exceeding 80% on average. High wind speed occurrences account for less than 1% of the annual total. Moreover, from December to February, the wind speeds are higher than the annual average and increase from 07:00 to 16:00. In addition, winter wind speeds are higher than summer wind speeds, and daytime wind speeds in all seasons are greater than those at night.

b. Wind Direction Analysis:

The annual average wind direction is predominantly northeast, accounting for over 57.51% of the distribution, followed by the southwest at 26.12%. Although the southwest wind reaches 66.14% in summer, the wind direction in summer is less stable; in winter, the northeast wind accounts for 97.43%, making it the most consistent directional flow.

c. Power Generation Analysis:

The data collected indicate that the overall annual net power generation is mostly low power generation (59.41%).

d. Seasonal Power Generation Analysis:

During summer, low net generation occurs 87.85%, while in winter, high net generation occurs 69.11% of the time. In summer, net power generation makes up 9.81% of the total annual output, while in winter, it accounts for 46.00% of the annual total.

e. Temporal Power Generation:

In winter, the power generation remains above 50% of the device capacity at all times, reaching a maximum of 80%. In contrast, the peak power generation in summer is only 17.82%.

f. Relationship between Power Generation and Wind Direction:

In winter, 99.87% of the power generation is produced by the northeast wind, whereas in summer, 70.82% is generated by the southwest wind.

g. Relationship between Power Generation and Wind Speed:

Annual wind speeds are concentrated between 2 (m/s) and 8 (m/s). As soon as the wind speed exceeds the turbine's cut-in speed of 3.5 (m/s), power generation increases significantly, demonstrating a positive correlation between wind speed and net power generation.

Due to the fact that Taiwan's offshore wind farms had not been completed at the time of data collection, the data used in this study were derived from an onshore wind power field. Although the characteristics of onshore wind power generation differ slightly from those of offshore wind power, the findings of this study provide sufficient reference evidence. Based on the analysis of the three key factors—wind speed, wind direction, and turbine power generation—it was determined that, although the southwest wind occurs in summer, its generally weak wind speeds are insufficient to provide stable long-term power generation during the summer peak. In contrast, the stable northeast wind in winter ensures relatively consistent power generation. However, since Taiwan experiences a peak in power demand during summer if wind power generation is unable to supply sufficient power to the grid during this period, the installation of additional energy storage systems becomes necessary. These systems would store excess wind power during periods of high generation, thereby mitigating the impact of low generation on the public grid and bridging the gap during the summer peak, ultimately enhancing the flexibility of power dispatch.

References

1. Tohbai Y, Wu G, Guo H. A basic study on construction and control of offshore wind power generation system. 2009 Transmission & Distribution Conference & Exposition: Asia and Pacific 2009. p. 1-4.
2. Liu J-H. Study on the Weather Impact of the Installation Schedule of Offshore Wind Farm Turbines in the Taiwan Strait. National Taiwan University; 2019.
3. Ren L, Ji J, Wang Y, Bu S, Lu Z, Luo X. Investigation into spatiotemporal

characteristics of coastal winds around the Taiwan Island. Energy Reports. 2022; 8:419-27.
4. Obara Sy, Fujimoto S, Sato K, Utsugi Y. Planning renewable energy introduction for a microgrid without battery storage. Energy. 2021; 215:119176.
5. Tooryan F, HassanzadehFard H, Collins ER, Jin S, Ramezani B. Smart integration of renewable energy resources, electrical, and thermal energy storage in microgrid applications. Energy. 2020; 212:118716.
6. Jin KM, Kim EH. Evaluating the impact of BESSs in the Jeju island power system. 2012 International Conference on Renewable Energy Research and Applications (ICRERA) 2012. p. 1-4.
7. Wang K-M, Kuo T-W, Hung S-P, Hsu J-Y, Sun C-H. The Study of the Optimal Operation of Electricity Market under the Electricity Liberalization Policy in Taiwan. Journal of Taipower's engineering. 2015; 805:61-81.
8. Chen H, Birkelund Y, Zhang Q. Data-augmented sequential deep learning for wind power forecasting. Energy Conversion and Management. 2021; 248:114790.
9. Shu ZR, Chan PW, Li QS, He YC, Yan BW. Investigation of chaotic features of surface wind speeds using recurrence analysis. Journal of Wind Engineering and Industrial Aerodynamics. 2021; 210:104550.
10. Jin H, Yang L, Gan J, Li Z, Li D, Chen S. Risk Assessment of Grid Frequency Deviation Related to Correlation Considering Wind Speed and Wind Direction in a Wind Farm. 2018 2nd IEEE Conference on Energy Internet and Energy System Integration (EI2) 2018. p. 1-5.
11. Wu M-T. The Applications of Artificial Neural Network to Wind Speed and Generation Forecasting of Wind Power System. National Kaohsiung University of Applied Sciences; 2008.
12. Ho L-S, Lin Ss, Chen C-H, Chiang M-L, Wei C-H, Luo G-S, et al. Analysis of 104 years of meteorological observations in Taiwan domestic sea commercial port waters Publication Abstracts of Research Projects Institute of Transportation Ministry of Transportation and Communications 2015.
13. Team RC. The R Project for Statistical Computing. 2025.

ISSN: 0067-3064

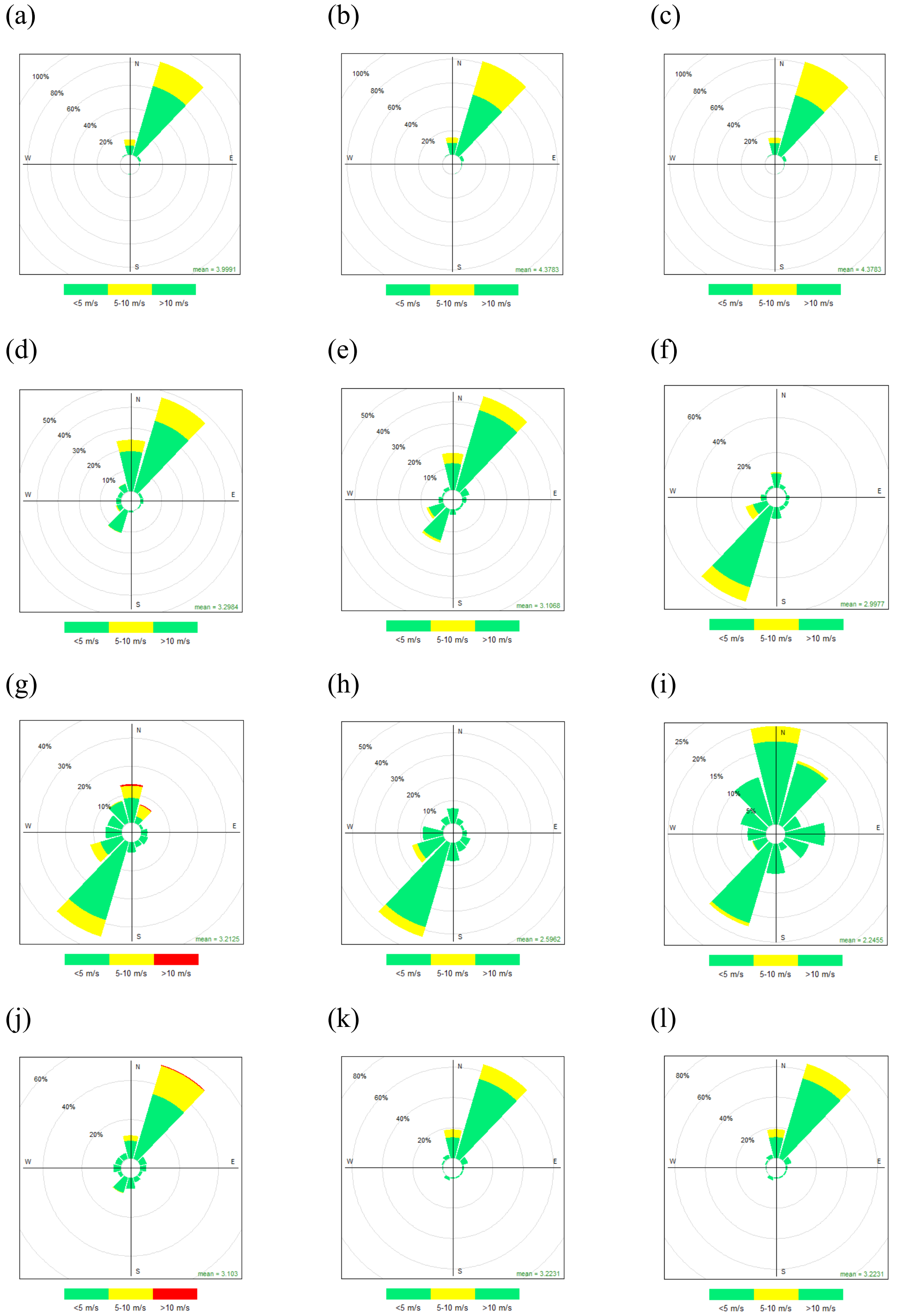

Supplement Fig. 1. Average wind speed rose diagram (a) Jan.; (b) Feb.; (c) Mar.; (d) Apr.; (e) May.; (f) Jun.; (g) Jul.; (h) Aug.; (i) Sep.; (j) Oct.; (k) Nov.; (l) Dec.

ISSN: 0067-3064

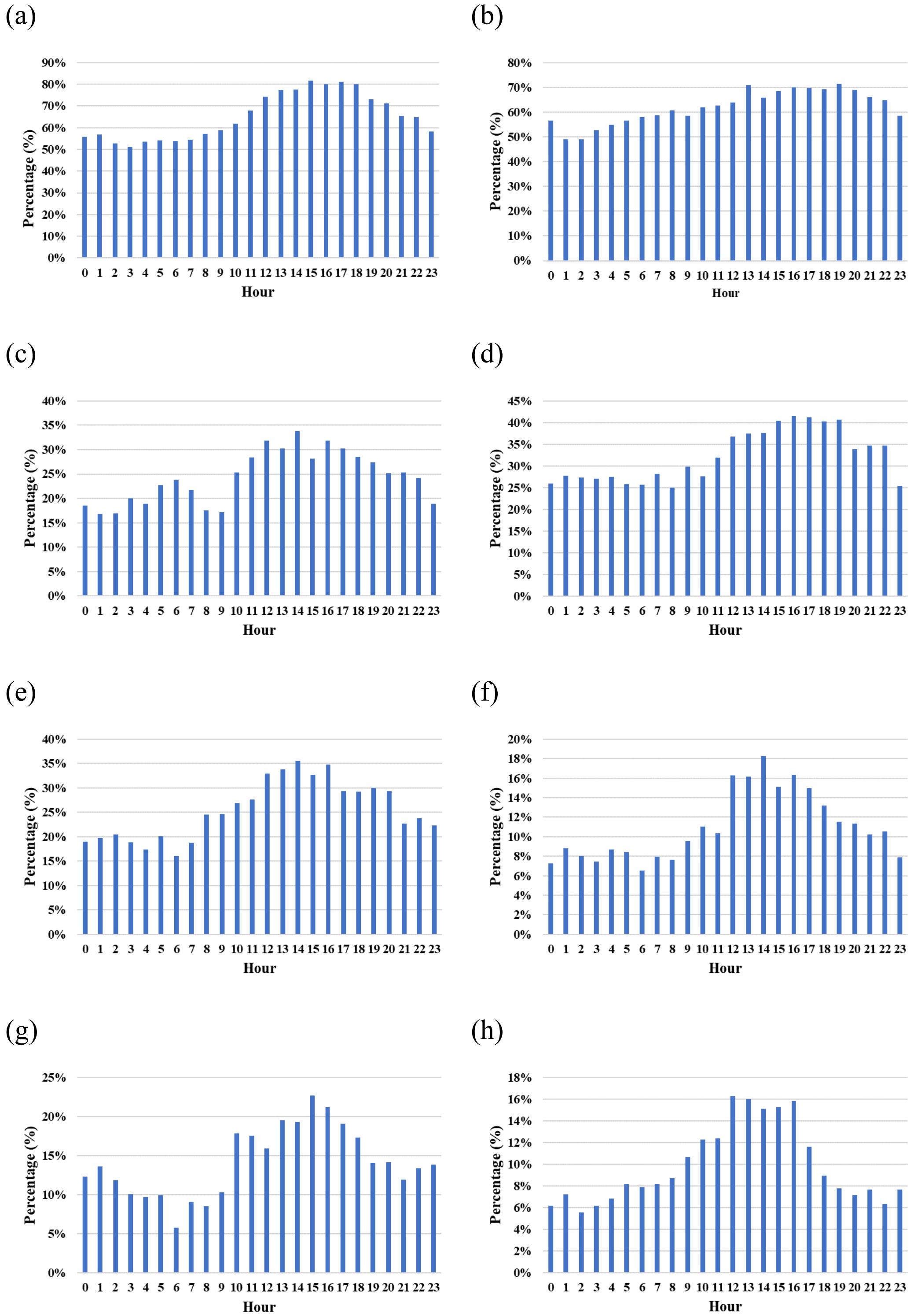

Supplement Fig. 2. Hourly average power generation percentage (a) Jan.; (b) Feb.; (c) Mar.; (d) Apr.; (e) May.; (f) Jun.; (g) Jul.; (h) Aug.

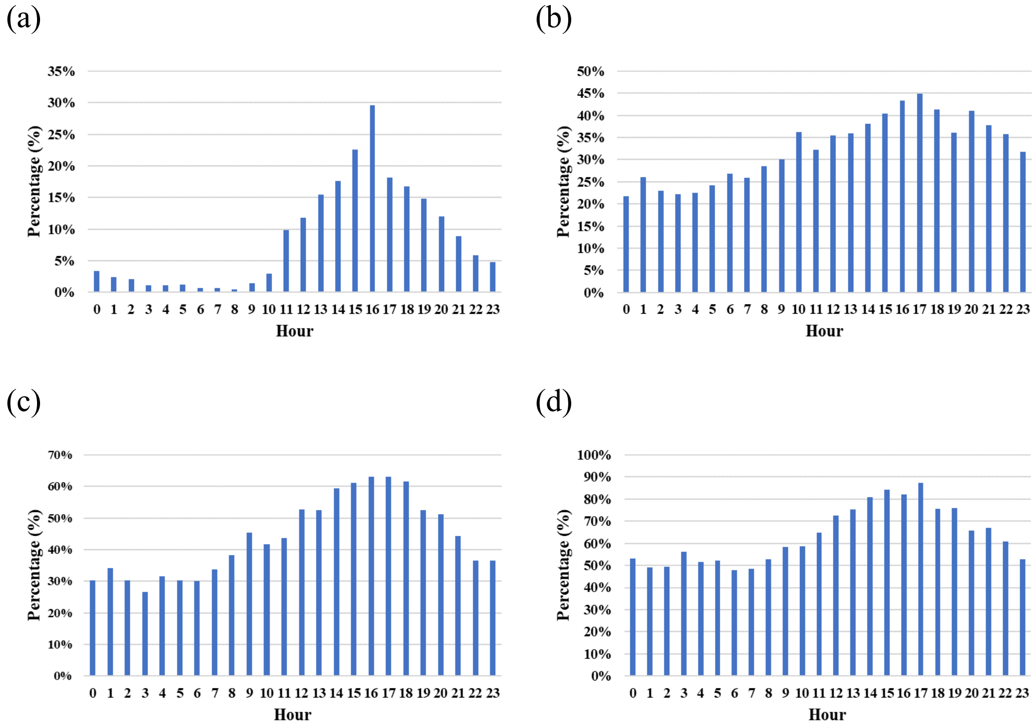

Supplement Fig. 3. Hourly average power generation percentage (a) Sep.; (b) Oct.; (c) Nov.; (d) Dec.